http://dx.doi.org/10.17159/2411-9717/2017/v117n10a6

# First-principles studies of Fe-Al-X (X = Pt, Ru) alloys

by C.S. Mkhonto, H.R. Chauke and P.E. Ngoepe


## Synopsis

**The Fe-Al based alloys have recently attracted a lot of attention due to their excellent resistance to oxidation at high temperatures. However, they suffer limited room temperature ductility and a sharp drop in strength above 600°C. The current study employed a density functional theory approach to investigate the stability of FeAl-X alloys. We employed virtual crystal approximation to model various atomic concentrations ($0 \leq X \leq 5$) of both Pt and Ru; this will allow more precise predictions on the materials' behaviour. Density of states was used to describe the behaviour of each phase near the Fermi level; these phases were observed at different percentage compositions. The FeAl composition is most favourable since it displays positive shear moduli, condition of mechanical stability. Addition of Pt and Ru was found to significantly improve the ductility of the Fe-Al-X compound for 0.2 and 0.5 at.% compositions, respectively.**



**Keywords**

**FeAl-X alloys, DFT, heats of formation, thermodynamic stability, density of states, elastic constants, X-ray diffraction patterns.**


## Introduction

The intermetallic iron-aluminium system has attracted a large amount of research since it possesses good mechanical properties, low density and low cost, as well as easy access to the raw materials (Couperthwaite, Cornish and Mwamba, 2016). It was also reported that the Fe-Al alloys are promising materials, due to their good refractoriness, oxidation and corrosion resistance and good ductility at room temperature (Couperthwaite, Cornish and Mwamba, 2016). However, these materials suffer limited room temperature ductility and a sharp drop in strength above 600°C, which makes them less suitable for use as structural materials (Li *et al.*, 2016).

Previous experimental work investigated the effect of precious metals (Pd, Ag, Ru, Pt) additions on the structure, oxidation and corrosion properties of a Fe-40 at.% Al (Fe-Al) alloy. It was reported that additions of more than 0.5 at.% precious metal did not improve the oxidation and corrosion properties of the materials and in some cases even decreased the resistance to corrosion (Couperthwaite Cornish and Mwamba, 2016; Li *et al.*, 2016). Four alloys were produced through mechanical alloying *i.e.* FeAl-0.2 at.% Pd, FeAl-0.2 at.% Ru, FeAl-0.5 at.% Ag, FeAl-0.5 at.% Pt. It was also found that the additions of Ru and Pt were crucial to the oxidation and corrosion properties, with Ru being considered the most favourable.

In previous work, it was established that additions of 0.2 at.% Ru to a Fe-40 at.% Al alloy improved the corrosion and oxidation resistance. Furthermore, the findings revealed that the non-equilibrium processing significantly refined the grain size of the material. The sintered material had a higher hardness than the as-cast material and the change in grain size did not significantly affect the oxidation and corrosion resistance (Chou *et al.*, 2006). Other research focused on the mechanically alloyed powder coated onto a mild steel substrate (approx. 5–10 μm thick) at a low gas pressure of 10 bar and temperature of 500°C. It was found that the coated materials effectively enhanced the oxidation and corrosion resistance (Chou *et al.*, 2006). Iron aluminides based on $Fe_3Al$ and FeAl are highly oxidation and corrosion resistant and have potential for elevated temperature structural applications (Kant *et al.*, 2016). Carbon is an important alloying element in $Fe_3Al$ as it increases strength and creep resistance, as well as resistance to environmental embrittlement (Colinet, 2003). However, addition of carbon to FeAl has not been successful as it leads to precipitation of graphite which causes decrease in strength (Colinet, 2003).


* *Materials Modelling Centre, School of Physical and Mineral Sciences, University of Limpopo, South Africa.*


 *ISSN 2225-6253. This paper was first presented at the* AMI Precious Metals 2017 Conference 'The Precious Metals Development Network' *17–20 October 2017, Protea Hotel Ranch Resort, Polokwane, South Africa.*

# First-principles studies of Fe-Al-X (X = Pt, Ru) alloys

In this study, DFT was used to investigate the structural, electronic and mechanical properties of Ru and Pt doped FeAl intermetallic. We employed the virtual crystal approximation (VCA) which allowed calculations on disordered systems to be carried out at the same cost as calculations for ordered structures (Ramer and Rappe, 2000). Small amounts of up to 0.5 at.% Pt and up to 0.2 at.% Ru were investigated to complement the previous experimental findings) (Couperthwaite, Cornish and Mwamba, 2016). The study modelled various atomic concentrations ($0 \leq X \leq 5$) of both Pt and Ru; to allow more precise predictions and understanding of the electronic and elastic behaviour of the FeAl compounds. The model is represented in Figure 1, showing possible doping of metal (M=Pt, Ru) atoms on either Al or Fe sublattices (Marker *et al.*, 2013; Inden and Pepperhoff, 1990).

## Computational methodology

Density functional theory (DFT) (Kohn and Sham, 1965) within generalised gradient approximation (GGA-PBE) exchange-correlation functional (Perdew, Burke and Ernzerhof, 1996) was used to study the Fe-Al alloys. We employed the plane wave pseudopotential method as implemented in CASTEP cod (Milman *et al.*, 1999; Hedin and Lundqvist, 1971). An energy cutoff of 500 eV was used, as it was sufficient to converge the total energy of the B2 FeAl phase. The Brillouin zone integrations were performed for suitably large sets of k-points. We used a 10 × 10 × 10 k-points before and after doping. In the calculation of elastic constants and density of states, a k-spacing of 0.2 was used. Optimisation of structural parameters (atomic positions and lattice parameters) was achieved by minimisation of forces and stress tensors. Initially, the optimised binary B2 FeAl structure gave equilibrium lattice parameter of 0.2852 nm, in good agreement with the experimental value of 0.2908 nm (Breuer *et al.*, 2001). The predicted heat of formation was -0.333 eV per atom compared to the experimental value of -0.376 eV per atom (Breuer *et al.*, 2001).

## Results and discussion

### *Effect of Ru and Pt on iron aluminides (FeAl)*

#### *Thermodynamic stability*

Figure 1 shows the binary B2 FeAl structure and VCA model doped with either Ru or Pt atoms. The metal concentration of 0.2 at.% Ru and 0.5 at.% Pt was considered (Couperthwaite, Cornish and Mwamba, 2016) to determine the structural and thermodynamic stability and to understand the electronic and elastic property signatures. Firstly, the most energetically favourable structure was determined by checking various metal doping concentrations on different sublattices as shown in Table I. The lattice parameter or volume mismatches for Pt and Ru were insignificant, since all the composition gave lattice parameters very close to one another (ranging between 0.280 nm and 0.290 nm). We have predicted that the Pt and Ru prefer the Fe sublattice with a composition of $Fe_{49.8}Al_{50}Ru_{0.2}$ and $Fe_{49.5}Al_{50}$ $Pt_{0.5}$. This analysis is deduced from the heats of formation of –0.455 eV and –0.431 eV per atom for Ru and Pt doping, respectively.

#### *Elastic constants*

In order to evaluate the elastic stability of the ternary systems, we calculated the elastic constants ($C_{ij}$) for $Fe_{50}Al_{49.8}Ru_{0.2}$, $Fe_{49.8}Al_{50}Ru_{0.2}$, $Fe_{50}Al_{49.5}Pt_{0.5}$, $Fe_{49.5}Al_{50}Pt_{0.5}$, $Fe_{49.9}Al_{49.9}Ru_{0.2}$ (50:50) and $Fe_{49.75}Al_{49.75}Pt_{0.5}$ (50:50) dopant at different concentrations as shown in Table I. Note that the symmetry was unchanged and only three independent elastic constants ($C_{11}$, $C_{12}$ and $C_{44}$) have been found for the cubic lattice. The mechanical stability criteria of cubic system (Mehl, Klein and Papaconstantopoulos, 1994) is given as:

$$C_{44} > 0, C_{11} > |C_{12}| \; ; \; C_{11} + 2C_{12} > 0$$

and shear is

$$G = \frac{1}{2}\left[\frac{C_{11} - C_{12} + 3C_{44}}{5} + \frac{5C_{44}(C_{11} - C_{12})}{4C_{44} + 3(C_{11} - C_{12})}\right]$$

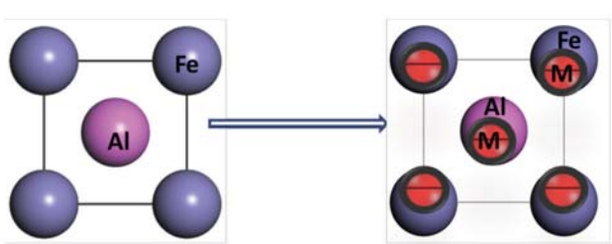


**Figure 1—Binary FeAl structural and VCA model showing metal (M: Ru or Pt) doping on Fe or Al sublattice**

*Table I*

**Equilibrium lattice parameters, volume and heats of formation ($\Delta H_f$) of the Fe-Al-X alloys**

| Composition | Dopant (at.%) | | Lattice parameter (nm) | Volume (nm³) | $\Delta H_f$ (eV per atom) |
|---|---|---|---|---|---|
| | Ru | Pt | | | |
| $Fe_{49.90}Al_{49.90}Ru_{0.2}$ | 0.2 | - | 0.2848 | 2.3107 | -0.453 |
| $Fe_{49.80}Al_{50}Ru_{0.2}$ | 0.2 | - | 0.2851 | 2.3185 | -0.455 |
| $Fe_{50}Al_{49.80}Ru_{0.2}$ | 0.2 | - | 0.2848 | 2.3108 | -0.452 |
| $Fe_{49.75}Al_{49.75}Pt_{0.5}$ | - | 0.5 | 0.2852 | 2.3220 | -0.429 |
| $Fe_{49.50}Al_{50}Pt_{0.5}$ | - | 0.5 | 0.2852 | 2.3197 | -0.431 |
| $Fe_{50}Al_{49.50}Pt_{0.5}$ | - | 0.5 | 0.2853 | 2.3220 | -0.427 |

All independent constants were positive and satisfied the stability conditions of the cubic lattice. Furthermore, the calculated shear moduli ($C'$) is positive, indicating the all compounds under considerations were elastically stable (Coudert and Mouhat, 2014). The elastic stability criteria also led to a restriction on the magnitude of $B$. Since $B$ is a weighed average of $C_{11}$ and $C_{12}$ and stability requires that $C_{12}$ be smaller than $C_{11}$, we are then left with the result that $B$ is required to be intermediate in value between $C_{11}$ and $C_{12}$: $C_{12} < B < C_{11}$. We predicted high values of $B$ for all systems with the lowest values corresponding to stable compounds. Thus, from the predicted $B$ values, we determined the ductility and brittleness of these compounds from the ratio of bulk to shear moduli. Pugh (1954) proposed the $B/G$ ratio predicted the ductility (> 1.75) or brittleness (< 1.75). For cubic Fe-Al alloys in Table II, we observed that $B/G < 1.75$, suggesting brittleness of the material. Note also that the negative values of $B/G$ also reflect instability of the corresponding compounds, which is not the case for the Fe-Al-X alloys. We noticed that the ductility is slightly enhanced for $Fe_{49.50}Al_{50}Pt_{0.5}$ and $Fe_{49.80}Al_{50}Ru_{0.2}$ systems (Breuer *et al.*, 2001).

### *Electronic DOS*

The electronic density of states (DOS) was calculated to mimic the stabilities by observing the behaviour of electronic states near the Fermi level. This approach has been used effectively in many studies and is mainly used to confirm or correlate the thermodynamic stability of intermetallic compounds (Mahlangu *et al.*, 2013; Phasha *et al.*, 2010). Firstly, we showed the total and partial density of states for the binary FeAl system in Figure 2a. We observed that the structure was characterised by a pseudogap near the Fermi level (confirming a metallic behaviour character). A more

*Table II*

**Elastic constants ($C_{ij}$) of the Fe-Al-X alloys**

| Structures | $C_{11}$ (GPa) | $C_{12}$ (GPa) | $C_{44}$ (GPa) | $C'$ (GPa) [1/2 ($C_{11}$–$C_{12}$)] | $G$ (GPa) | $B$ (GPa) | $B/G$ (GPa) |
|---|---|---|---|---|---|---|---|
| $Fe_{49.90}Al_{49.90}Ru_{0.2}$ | 283.0 | 141.4 | 148.3 | 212.3 | 110.219 | 187.892 | 1.705 |
| $Fe_{49.80}Al_{50}Ru_{0.2}$ | 279.4 | 140.6 | 147.4 | 209.1 | 108.942 | 186.885 | 1.715 |
| $Fe_{50}Al_{49.80}Ru_{0.2}$ | 282.2 | 140.7 | 148.2 | 211.8 | 110.144 | 188.590 | 1.712 |
| $Fe_{49.75}Al_{49.75}Pt_{0.5}$ | 282.5 | 147.9 | 147.9 | 208.5 | 107.828 | 187.304 | 1.737 |
| $Fe_{49.50}Al_{50}Pt_{0.5}$ | 278.9 | 139.9 | 147.5 | 208.9 | 101.799 | 186.243 | 1.707 |
| $Fe_{50}Al_{49.50}Pt_{0.5}$ | 282.0 | 139.3 | 147.9 | 212.4 | 103.487 | 186.917 | 1.693 |

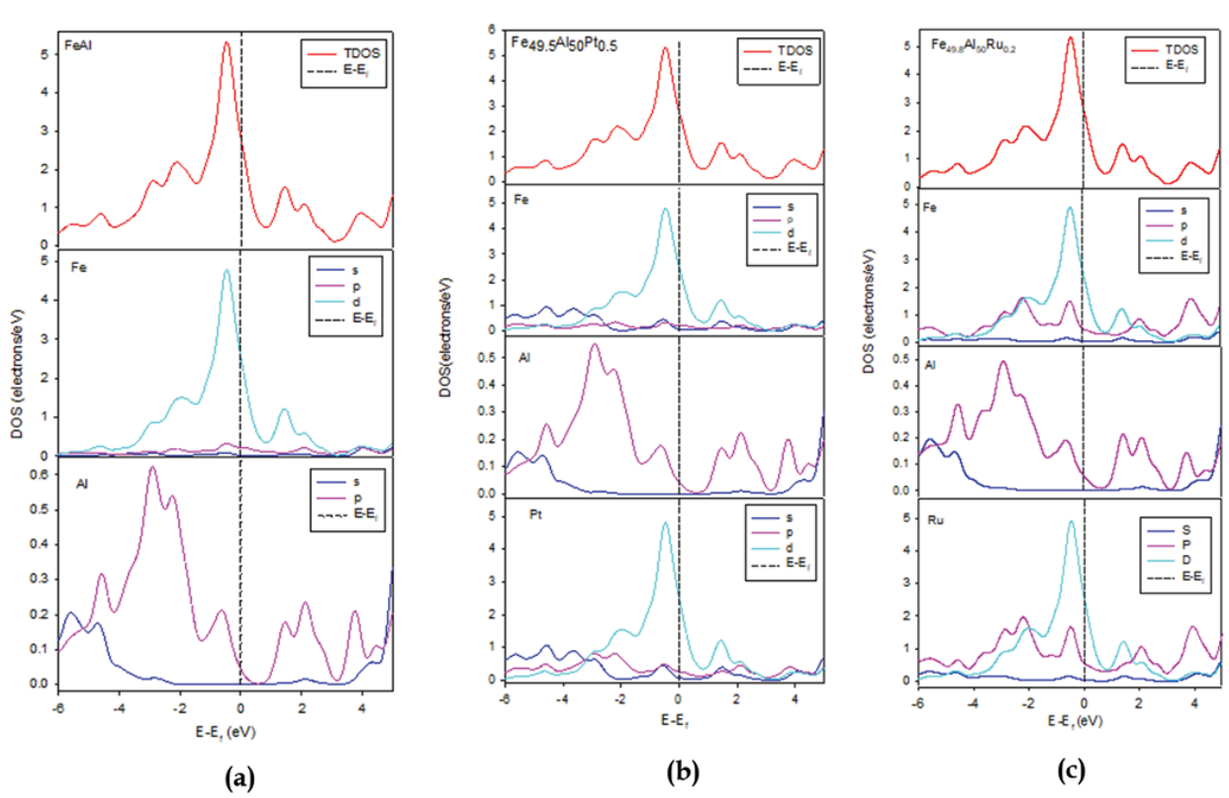


**Figure 2—Total and partial density of states of (a) binary FeAl and ternary (b) $Fe_{49.5}Al_{50}Pt_{0.5}$ and (c) $Fe_{49.8}Al_{50}Ru_{0.2}$ systems, with the Fermi energy taken as energy zero ($E$-$E_f$ = 0)**

noticeable Fe *d*-peak was observed, which forms a strong hybridisation with the Al *p*-orbital. More importantly, we see that the Fermi level fell slightly on the left of the pseudogap, which signifies electronic stability in agreement with the predicted heats of formation (*i.e.* good correlation).

### *Ternary system (DOS)*

Figures 2b and 2c show the total and partial density of states for $Fe_{49.5}Al_{50}Pt_{0.5}$ and $Fe_{49.8}Al_{50}Ru_{0.2}$, respectively. It is clear from the plot that doping with Pt and Ru slightly changed the behaviour of the electronic structure, in particular, shifting of the Fermi level with respect to the pseudogap. Note that the two plots show 0.5 at.% Pt and 0.2 at.% Ru doped on the Fe sublattice, noticeably the partial DOS for Al, were similar (row 2 of Figures 2b and 2c), while those for Fe/Pt (in Figure 2b) and for Fe/Ru (in Figure 2c) were different. A small peak at about –0.5 eV was sharper for the Ru-doped system than for Pt. More importantly, we noticed that the Fermi level slightly fell in the pseudogap (at $E–E_F = 0$) for both 0.5 at.% Pt and 0.2 at.% Ru, similar to the binary phase (Figure 2a).

Accordingly, doping with Pt on the Fe sublattice would be a preference for the given concentration, since it is more stable. The total and partial DOS for the doped structures are compared in Figure 3. We observed similar trends as those in Figure 2, the plots only shows significant difference with the appearance of peaks at about –-0.5 eV, which was attributed to either Pt or Ru additions.

### *XRD analysis*

We observed the X-ray diffraction patterns for binary FeAl and the stable compounds ($Fe_{49.5}Pt_{0.5}$ and $Fe_{49.8}Al_{50}Ru_{0.2}$), as shown in Figure 4. These plots displayed similar peaks before and after doping. However, the intensity of doped Ru system was very similar to the binary FeAl phase. Most notable was the high intensity peak at about 32 a.u and 70 a.u. This XRD pattern confirmed the structure and the fact that it did not change was attributed to the small amounts of Pt and Ru that dissolved into the structure.

## Summary and conclusion

The equilibrium lattice parameter, heats of formation, elastic

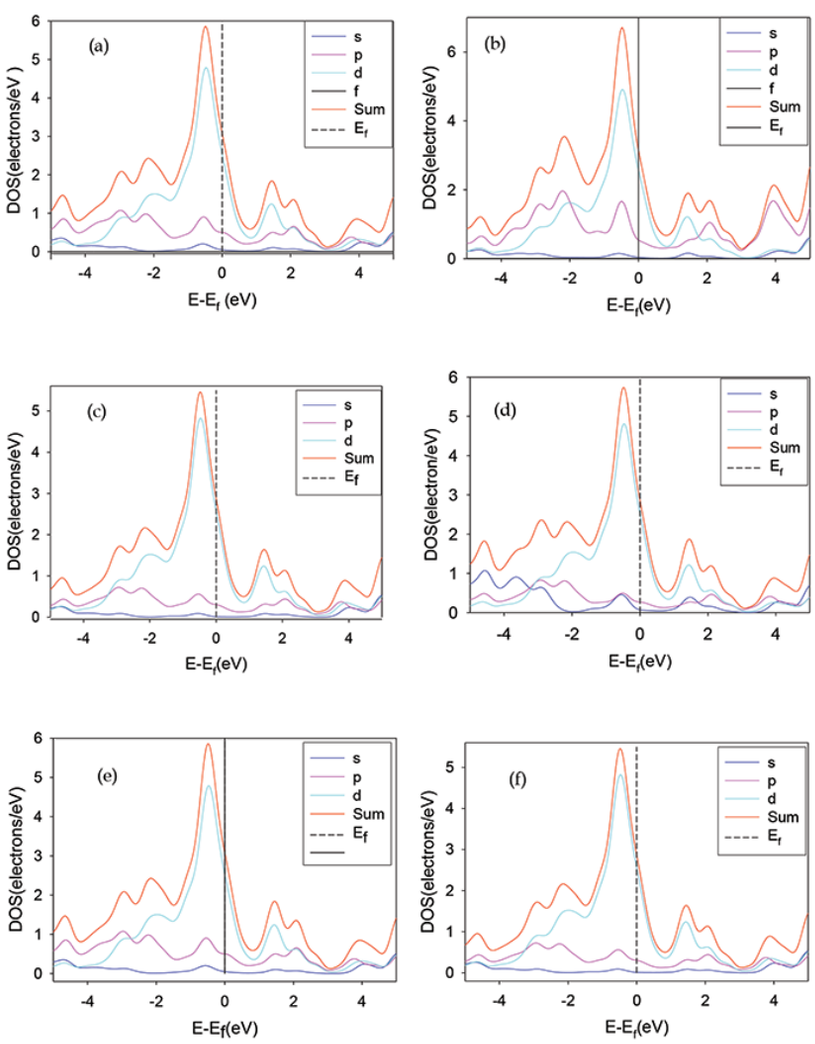


**Figure 3—Total and partial density of states of FeAl after doping: (a) $Fe_{50}Al_{49.8}Ru_{0.2}$, (b) $Fe_{49.8}Al_{50}Ru_{0.2}$, (c) $Fe_{50}Al_{49.5}Pt_{0.5}$, (d) $Fe_{49.5}Al_{50}Pt_{0.5}$, (e) $Fe_{49.9}Al_{49.9}Ru_{0.2}$ and (f) $Fe_{49.75}Al_{49.75}Pt_{0.5}$ with Fermi energy taken as the energy zero ($E$-$E_f$ = 0)**

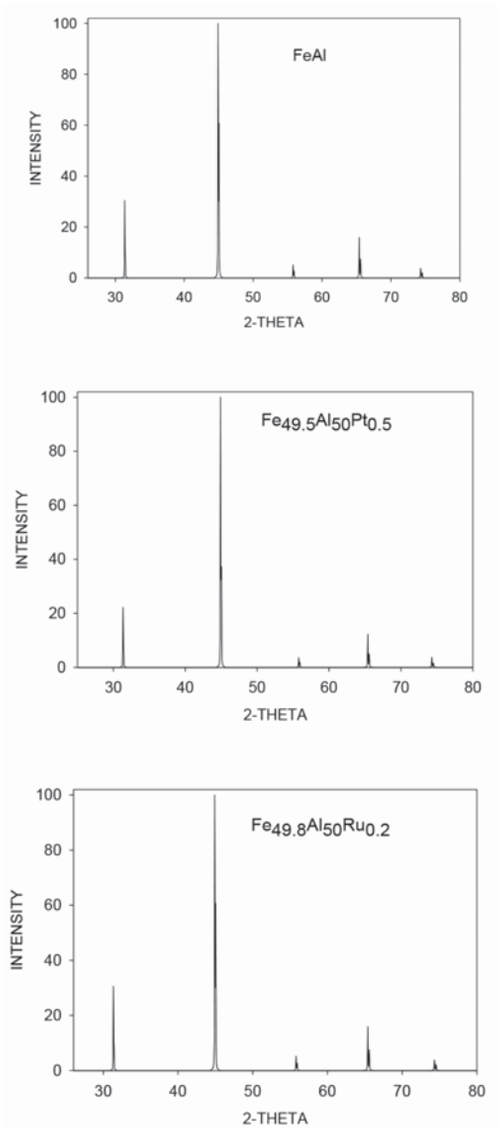


**Figure 4—XRD patterns of binary FeAl and doped $Fe_{49.5}Al_{50}Pt0.5$ and $Fe_{49.8}Al_{50}Ru_{0.2}$**

properties and electronic structure of the B2 FeAl phase were determined using *ab initio* calculations. Interestingly, the B2 FeAl at 50:50 was found to be energetically and mechanically stable over the other phases at different compositions. These phases exist in the range between 23 and 55 atomic percent Al of the experimental phase diagram (Atabaki *et al.*, 2014). The shear modulus (C') of the B2 FeAl phase was found to be positive, fulfilling the condition of stability. The DFT results were in good agreement with the experimental findings (Couperthwaite, Cornish and Mwamba, 2016). It was found that the FeAl structure was more stable (lowest heats of formation) and VCA showed preference of doping on Fe rather than Al sublattices: $Fe_{48.8}Al_{50}Ru_{0.2}$ and $Fe_{49.5}Al_{50}Pt_{0.5}$; and finally the DOS showed that the Fermi level fell in the pseudogap which demonstrates the condition of stability.

## Acknowledgement

The work was carried at the Materials Modelling Centre, University of Limpopo. The support of the South African Research Chair Initiative of the Department of Science and Technology and the National Research Foundation is highly appreciated.

## References

Atabaki, M.M., Nikodinovski, M., Chenier, P., Ma, J., Harooni, M. and Kovacevic R. (2014). Welding of aluminium to steels: an overview. *Journal for Manufacturing Science and Production*, vol. 14. pp. 2191–4184.

Breuer, J., Grün, A., Sommer, F. and Mittemeijer, E.J. 2001. Enthalpy of formation of B2-Fe1–xAlx and B2-(Ni,Fe)1–xAlx. *Metallurgical and Materials Transactions B*, vol. 32. pp. 913–918.

Chou, S., Huang, J., Lii, D. and Lu, H. 2006. The mechanical properties of $Al_2O_3$/aluminum alloy A356 composite manufactured by squeeze casting. *Journal of Alloys and Compounds*, vol. 419. pp. 98–102.

Colinet, C. 2003. ab-initio calculation of enthalpies of formation of intermetallic. *Intermetallics*, vol. 11. pp. 1095–1102.

Couperthwaite, R.A., Cornish, L.A. and Mwamba, I.A. 2016. Cold-spray coating of Fe-40 at. % Al alloy with additions of ruthenium. *Journal of the Southern African Institute of Mining and Metallurgy*,vol. 116. pp. 927–934.

Hedin, L. and Lundqvist, B.I. 1971. Explicit local exchange-correlation potentials. *Journal of Physics C: Solid State Physics*, vol. 4. pp. 2064–2082.

Inden, G. and Pepperhoff, W. 1990. Experimental study of the order: disorder transition in bcc Fe-Al alloys. *Zeitschrift für Metallkunde*, vol. 81. pp. 770–773.

Kant, R., Prakash, U., Agarwala, V. and Stya Prasad, V.V. 2016. Effect of carbon and titanium additions on mechanical properties of B2 FeAl. *Transactions of the Indian Institute of Metals*, vol. 69. pp. 845–850.

Kohn, W. and Sham, L.J. 1965. Self-consistent equations including exchange and correlation effects. *Physical Review*, vol. 140. pp. 1133–1138.

Li, X., Scherf, A., Heilmaier, M. and Stein, F. 2016. The Al-rich part of the Fe-Al phase diagram. *Journal of Phase Equilibria and Diffusion*, vol. 39. pp. 162–173.

Mahlangu, R., Phasha, M.J., Chauke, H.R. and Ngoepe, P.E. 2013. Structural, elastic and electronic properties of equiatomic PtTi as potential high-temperature shape memory Alloy. *Intermetallics*, vol. 33. pp. 27–32.

Marker, M.C.J., Duarte, L.I., Leinenbach, C. and Richter, K.W. 2013. Characterization of the Fe-rich corner of Al-Fe-Si-Ti. *Intermetallics*, vol. 39. pp. 38–49.

Mehl, M.J., Klein, B.M. and Papaconstantopoulos, D.A. (1994). Principles. *Intermetallic Compounds*, vol. 1. Westbrook J.H. and Fleischer R.L. (eds.). Wiley.

Milman, V., Winkler, B., White, J.A, Pickard, C.J., Payne, M.C., Akhmatskaya, E.V. and Nobes, R.H. 1999. Electronic structure, properties, and phase stability of inorganic crystals: a pseudopotential plane-wave study. *International Journal of Quantum Chemistry*, vol. 77. pp. 895–910.

Mouhat, F. and Coudert, F. 2014. Neccesary and sufficient elastic conditions in various crystal systems. *Physical Review B*, vol. 90. pp. 224104–224107.

Perdew, J.P., Burke, K. and Ernzerhof, M. 1996. Generalized gradient approximation made simple. *Physical Review Letters*, vol. 77. pp. 3865–3868.

Phasha, M.J., Ngoepe, P.E., Chauke, H.R., Pettifor, D.G. and Nguyen-Mann, D. 2010. Link between structural and mechanical stability of fcc- and bcc-based ordered Mg-Li alloys. *Intermetallics*, vol. 18. pp. 2083–2089.

Pugh, S.F. 1954. XCII. Relations between the elastic moduli and the plastic properties of polycrystalline pure metals. *The London, Edinburgh, Dublin Philosophical Magazine and Journal of Science*, vol. 45, no. 367. pp. 823–843.

Ramer, N.J. and Rappe, A.M. 2000. Application of a new virtual crystal approach for the study of disordered perovskites. *Journal of Physics and Chemistry of Solids*, vol 61. pp. 315–320. ◆